

An exploratory efficacy study of the amyloid imaging agent [¹⁸F]flutemetamol in Japanese Subjects

Michio Senda · Yasuji Yamamoto · Masahiro Sasaki ·
Tomohiko Yamane · David J. Brooks ·
Gill Farrar · Brian McParland · Kerstin Heurling

Received: 14 October 2014 / Accepted: 29 January 2015 / Published online: 10 February 2015
© The Japanese Society of Nuclear Medicine 2015

Abstract

Aim The aim of the study presented was to investigate the brain uptake properties of the amyloid PET agent [¹⁸F]flutemetamol in Japanese healthy controls and clinically probable Alzheimer's disease (AD) patients, and to make a comparison with the results of a previously performed study on Caucasian subjects. [¹⁸F]flutemetamol was recently approved by the American Food and Drug Administration and the European Medicines Agency for visualization of amyloid in vivo. Since the first clinical study of [¹⁸F]flutemetamol—an ¹⁸F

derivative of the PET tracer 11C-Pittsburgh Compound B targeting β-amyloid—took place, several clinical studies have been performed, but few focusing on a Japanese population.

Methods In the Step A, three elderly healthy volunteers and three AD subjects underwent dynamic PET scanning 0–30 and 60–150 min after injection of 185 MBq [¹⁸F]flutemetamol. The brain volume of distribution (V_T) was quantified using Logan's linear graphical analysis and as standardized uptake value ratios (SUV_R) with a cerebellar reference. The optimal acquisition window was determined from brain time activity curves for Step B. In the Step B, 5 AD and 5 elderly healthy volunteers were scanned from 80 to 140 min after intravenous injection of [¹⁸F]flutemetamol. The data from the two parts were pooled for estimation of overall efficacy.

Results [¹⁸F]Flutemetamol injection was shown to be safe—no serious adverse events were reported during this study. A simplified SUV_R estimate of the uptake of [¹⁸F]flutemetamol using a time window of 85–115 min post injection successfully discriminated AD cases from healthy volunteers. AD subjects showed an elevated tracer uptake in prefrontal cortex, the lateral temporal cortex and precuneus amongst other regions. No significant [¹⁸F]flutemetamol PET differences could be seen between the Japanese AD cases in this study and those from an earlier Caucasian study, or between control subjects in Japanese and Caucasian studies.

Conclusions This study supports the use of [¹⁸F]flutemetamol PET in Japanese population as a marker of the presence of fibrillar β-amyloid. The lack of differences between the Japanese cohort and those from a previous Caucasian cohort supports the extrapolation of results from other Caucasian [¹⁸F]flutemetamol PET studies to the Japanese population.

M. Senda · M. Sasaki · T. Yamane
Division of Molecular Imaging, Institute of Biomedical Research
and Innovation, Kobe, Japan

Y. Yamamoto
Department of Psychiatry, Kobe University Hospital, Kobe,
Japan

D. J. Brooks
Department of Medicine, Imperial College, London, UK

D. J. Brooks
Department of Nuclear Medicine and PET-Centre, Aarhus
University, Aarhus, Denmark

G. Farrar · B. McParland
Life Sciences, GE Healthcare, Amersham, UK

K. Heurling (✉)
Life Sciences, GE Healthcare, Björkgatan 30, 75184 Uppsala,
Sweden
e-mail: kerstin.heurling@radiol.uu.se

K. Heurling
Nuclear Medicine and PET, Department of Surgical Sciences,
Uppsala University, Uppsala, Sweden

Keywords [^{18}F]flutemetamol · Alzheimer's disease · Amyloid β · Japanese population · Positron emission tomography

Introduction

Japan has one of the world's highest ratios of elderly to the total population and, as the population keeps growing older, diseases associated with aging are becoming a serious medical and economic problem. The prevalence of dementia within the Japanese population has increased over the last decades, with a report of threefold increase in prevalence between 1985 and 2005 among the Japanese elderly [1]. In 2010, the estimated number of people suffering from dementia in Japan was 2.5 million. Approximately, 35.6 million worldwide are estimated to suffer from dementia, a number that is expected to double every 20 years reaching over 115 million in 2050 [2].

The presence of neuritic β -amyloid plaques in brain tissue is a pathological hallmark of Alzheimer's disease (AD). PET imaging agents that can visualize fibrillar β -amyloid have been developed by a number of investigators. Among them, [^{18}F]flutemetamol has recently been approved by the American Food and Drug Administration (FDA) and the European Medicines Agency (EMA) as a diagnostic agent for visualization of amyloid (VizamyliTM, GE Healthcare).

[^{18}F]Flutemetamol is a fluorine-18 derivative of the carbon-11 labeled Pittsburgh Compound B ([^{11}C]PiB), which is a neutral analog of thioflavin T, an accepted histological stain for detecting amyloid fibrils. Because the half-life of fluorine-18 (110 min) is longer than that of carbon-11 (20 min), [^{18}F]flutemetamol offers more flexibility in distribution and in scheduling of PET imaging. The first clinical study of [^{18}F]flutemetamol was conducted in Caucasian healthy volunteers and subjects with clinically probable AD based on National Institute of Neurological and Communicative Disorders and Stroke, the Alzheimer's Disease and Related Disorders Association and the Diagnostic and Statistical Manual of Mental Disorders, 4th ed (NINCDS-ADRDA DSM-IV) criteria [3] with the aim to investigate dosimetry, biodistribution, brain kinetics, optimal imaging window, methodology for analysis and differences in brain retention between AD patients and healthy controls [4, 5]. Studies that followed investigated the efficacy of [^{18}F]flutemetamol for detecting amyloid in mild cognitive impairment [6, 7] and compared PET findings against a standard of truth of histopathology [8, 9]. However, few clinical studies have been reported on the Japanese population [10].

The aim of the present study was to investigate [^{18}F]flutemetamol brain uptake in Japanese healthy controls and clinically diagnosed AD patients, and to make a comparison with the results of a previously performed study on Caucasian subjects [4].

Materials and methods

Subjects

The original study was performed in three parts, with the first part being a dosimetry assessment which is being published separately (submitted). The second part (herein referred to as Step A) included a cohort of three elderly healthy volunteers (HV) and three patients with probable Alzheimer's disease (AD) looking at the brain kinetics of [^{18}F]flutemetamol. The third part (herein referred to as Step B) included five HV subjects and five AD patients looking at the efficacy and optimal scanning window of [^{18}F]flutemetamol. The patients were registered at Kobe University Hospital and the healthy volunteers were recruited at the Institute of Biomedical Research and Innovation (IBRI) in Kobe, Japan. The average age of the entire study population was 66.8 years with an age range of 54–90 years. Eight men and eight women were included in the study. Each study subject underwent an assessment of his/her cognitive ability. The AD patients fulfilled the criteria of NINCDS-ADRDA. Their Mini-Mental State Examination (MMSE) score had to be between 18 and 26, a Clinical Dementia Rating of 0.5, 1 or 2 and a Modified Hachinski Ischemia score ≤ 4 to be included in the study. For the healthy volunteers the MMSE had to be ≥ 27 and they must not be complaining of cognitive impairment or have more than one first degree relative with a diagnosis of AD. Demographics and neuropsychological status of the participants are summarized in Table 1.

Written informed consent was obtained from each subject included in the study prior to any study-related procedures, in accordance with the Declaration of Helsinki. The study was approved by the local independent ethics committees.

Radiochemistry and imaging procedures

Radiochemistry

The investigational medicinal product Flutemetamol F 18 Injection was synthesized and purified by solid-phase extraction on a FASTlab platform (GE Healthcare), prepared and handled according to good manufacturing practice at the manufacturing site at IBRI. Each batch was delivered to the imaging site at IBRI accompanied by a delivery sheet

Table 1 Demographics and neuropsychological status

	Mean	SD	Range
Healthy volunteers (HV) ($N = 8$, M/F = 5/3)			
Age	58.9	3.3	54, 62
Body weight	61.8	9.8	46.7, 73.8
MMSE	28.9	0.6	28, 30
Patients with probable Alzheimer's disease (AD) ($N = 8$, M/F = 3/5)			
Age	74.6	10.2	62, 90
Body weight	58.5	8.2	51.9, 78.0
MMSE	23.1	2.9	18, 26
CDR	0.94	0.18	0.5, 1
Word list learning	6.6	1.4	4, 8
Word delayed recall	9.9	0.4	9, 10
Word list recognition	5.0	1.8	4, 9
Digit span forward	7.6	1.5	5, 10
Digit span backward	4.9	1.6	2, 7
Animal verbal fluency	10.5	2.3	6, 12
Letter verbal fluency	19.6	11.0	5, 39
Boston naming test (30 items)	21.4	6.6	8, 27
Trail making test part A (s)	73	48	31, 150
Trail making test part B (s)	191	81	114, 300

with detailed batch specifics. At the imaging site, Flutemetamol F 18 Injection was injected intravenously as a bolus dose (<40 s) via the antecubital vein, with a total flutemetamol amount <10 μ g. The average administered dose was 188.4 MBq, range 182.2–197.5 MBq.

MR acquisition

MRI images for AD patients were acquired with a Philips Achieva 1.5T Nova Dual MR scanner at Kobe University Hospital. The scanning included 3D- T_1 (GR, TE = 1.88 ms, TR = 6.72 ms, Flip angle = 9, matrix = 256, FOV = 230 mm, 190 slices, slice thickness = 0.9 mm) as well as axial T_2 (SE), FLAIR and DWI in 2D.

MRI images for HV were acquired with a GE 1.5T Signa Excite MR scanner at IBRI. The scanning included 3D- T_1 (FAST SPGR, TR = 10.3 ms, TE = “minimum full”, flip angle = 8, matrix = 224, FOV = 240 mm, 252 slices, slice thickness = 1 mm) which was used for co-registration of the PET images, as well as axial T_1 (SE), T_2 (FSE) and FLAIR in 2D.

The MRI data was used as part of the screening process to exclude for lesions and anatomical abnormalities as well as for anatomical volume-of-interest (VOI) definition during processing and analysis of the PET image data.

PET acquisition

All subjects underwent dynamic PET scanning on a Siemens EXACT ECAT HR + PET scanner. For subjects

included in Step A the scanning started at the administration of Flutemetamol F 18 Injection, and lasted for 30 min to properly capture the blood flow component of the tracer uptake. The subjects were allowed to leave the scanner bed for a short rest 30–60 min post-injection (p.i.) and were then repositioned in the gantry when the scanning was resumed at 60 min and lasted until 150 min post-injection. Before each of the two PET scans a ^{68}Ge transmission scan was performed to allow attenuation correction during the reconstruction. The dynamic data was collected as 5-min frames.

In Step B, the scanning protocol was simplified and scanning started at 80 min post-Flutemetamol F 18 Injection administration and lasted 50 min, collected as 5-min frames enabling re-binning and inter-frame motion correction, preceded by a ^{68}Ge transmission scan.

Image processing

The data was reconstructed using 2D ordered subsets expectation maximization. During the reconstruction corrections for tissue attenuation, random counts and scatter were applied. The dynamic images were corrected for possible patient movement using a frame-to-frame realignment, with the first frame as reference image. Dynamic PET data for each subject were co-registered to the MR T_1 -weighted data and both PET and MR data were transformed into Montreal Neurological Institute (MNI) template space using a polynomial non-linear registration [11] of the

subject's MRI data to the MNI MR T₁ template to allow for application of the predefined template VOIs in MNI space. The image processing was performed using VOIager software (version 4, GE Healthcare, Uppsala, Sweden).

VOI analysis

The predefined template VOIs used for quantification of uptake of [¹⁸F]flutemetamol included the bilateral delineations of frontal cortex, anterior cingulate, medial temporal cortex, lateral temporal cortex, inferior parietal cortex, sensorimotor cortex, occipital cortex, striatum, subcortical white matter, precuneus and posterior cingulate, as visualized in Fig. 1. A composite VOI combining the uptake of frontal cortex, lateral temporal cortex, anterior cingulate, inferior parietal cortex and precuneus and posterior cingulate to represent the global cortical uptake was also used in the analysis. Regions generally unaffected by β -amyloid accumulation, previously defined as valid reference regions [4] were also part of the VOI template, including cerebellar cortex as the primary and pons as the secondary reference region. The VOIs were applied to the template space dynamic PET data producing time-activity curves for all the included regions.

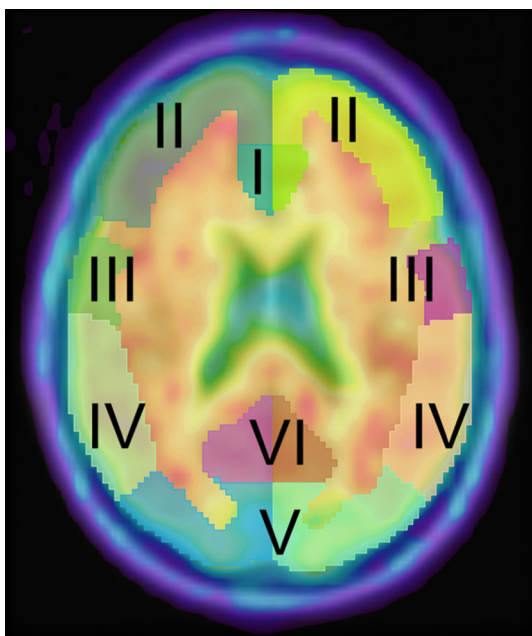


Fig. 1 Examples of pre-defined VOIs used in the analysis shown at the level of anterior cingulate and posterior cingulate on a representative positive [¹⁸F]flutemetamol image shown as an overlay on a T₁ MRI template; *I* anterior cingulate, *II* frontal cortex, *III* sensorimotor cortex, *IV* inferior parietal cortex, *V* occipital cortex, *VI* posterior cingulate and precuneus

Graphical analysis of Step A Data

A previously performed phase I study of [¹⁸F]flutemetamol [4] evaluated use of reference region based models for quantification of the uptake, showing that the distribution volume (V_T) computed with plasma input 2-tissue compartment modeling [12] correlated well with the distribution volume ratio (DVR) estimated using plasma input based graphical analysis using the Logan plot [13], and that Logan DVR using a plasma input correlated well with reference tissue Logan graphical analysis DVR [14] for data collected from 60 min post-injection with the cerebellar cortex as reference region. In this Japanese study, only the reference Logan model was used.

Standardized uptake value ratio (SUVR) analysis

A simplified method for quantifying PET data was applied to Step A and Step B data. This method is based on estimating the ratio between the VOI activity uptake over a defined time window compared with a reference region of non-specific binding. The resulting estimate, called an SUVR, is commonly used for quantification of amyloid PET tracers [4, 15–17]. When performing the ratio operation, effects of subject body weight and potential differences in administered dose are automatically removed. Utilizing the common imaging windows in Steps A and B (80–130 min p.i.) allows for the analysis of pooled data.

Statistical analysis

The relationships between graphical Logan estimated DVRs and SUVRs were evaluated through least-squares linear regression of the Step A data. A mean of the Pearson's correlation coefficient (r) for the studied regions was calculated as an indicator of the strength of correlation. Differences in mean regional SUVR between HV and AD subjects were evaluated using Student's t test with $p = 0.05$ as a threshold for significance, assessing the discriminating abilities of [¹⁸F]flutemetamol.

Population-based comparisons

To assess any differences in the uptake of [¹⁸F]flutemetamol between Japanese and Caucasian populations, comparisons of SUVR measurements in the composite VOI and the five cortical regions comprising it, was performed between subjects in this study and those described by Nelissen et al. [4]. In the latter historical study, the ethnicity was confirmed to be Caucasian for all subjects through review of clinical trial records. The historical study had the same overall design, although with slightly

different scanning windows. The common scanning window for all subjects was 80–90 min p.i and therefore, the comparison between the populations was performed on this window. Two group comparisons were made, the first comparing the Japanese AD subjects ($n = 8$) with the Caucasian AD subjects ($n = 8$) and the second comparing the Japanese HV subjects with the Caucasian HV subjects in a separate analysis. Student's two-tailed t test was applied using homoscedastic variance. Image data for the Caucasian cohort were re-analysed for this comparison using the same image processing and VOI definition as for the Japanese cohort.

Results

No serious adverse events related to administration of Flutemetamol F 18 Injection were recorded for the 16 participating subjects.

Tracer uptake over time

The brain uptake of [^{18}F]flutemetamol was plotted as time activity curves and averaged for the three healthy volunteers and three AD subjects in Step A. Examples of these curves for the VOIs sampling precuneus and posterior cingulate, frontal cortex, white matter, cerebellar cortex and pons are shown in Fig. 2a. The time-activity curves indicate that the healthy volunteers and AD subjects had similar tracer uptake in pons and cerebellum but the AD cohort showed increased uptake in frontal cortex, precuneus and posterior cingulate. This is also evident in Fig. 2b where region:cerebellar cortex uptake ratios (SUVR) for precuneus and posterior cingulate, frontal cortex, and pons are plotted against time. The graph shows

greater increases in SUVR of the cortical VOIs covering frontal cortex and posterior cingulate and precuneus over time in the AD group compared with the HV group. There is no visible difference between the pons SUVR between healthy volunteers and AD subjects.

Quantitative analysis of step A data

The distribution volume ratios (DVRs) obtained using cerebellar reference-based plots are listed in Table 2 for the Step A subjects. The graphical model was applied to the 60–150 min time window. It produced a linear relationship with high correlation coefficients ($r = 1.00$). Table 2 also lists the SUVR values for each subject and region using cerebellar cortex as the reference region for the 85–115 min time window. Finally, the correlation of the two quantification methods is shown in Fig. 3, proving a high correlation with a correlation coefficient of $r = 0.97$. These data establish the use of a 30 min scanning window and a snapshot SUVR as an appropriate simplification of a full dynamic imaging method for quantifying the uptake of [^{18}F]flutemetamol.

Group comparisons of in the pooled step A and B data

Discriminating abilities of [^{18}F]flutemetamol PET were investigated by pooling all subjects from Step A and Step B, resulting in eight healthy subjects and eight with clinically probable AD. Figure 4 shows summation images for all subjects from Step A and B, in axial and sagittal view for a summation covering 85–115 min, with the intensity anchored by setting the pons to 90 % of maximum on the image intensity scale. The visual uptake profile shows an increased level of intensity in the cortical regions for the AD subjects compared to the HV subjects, except

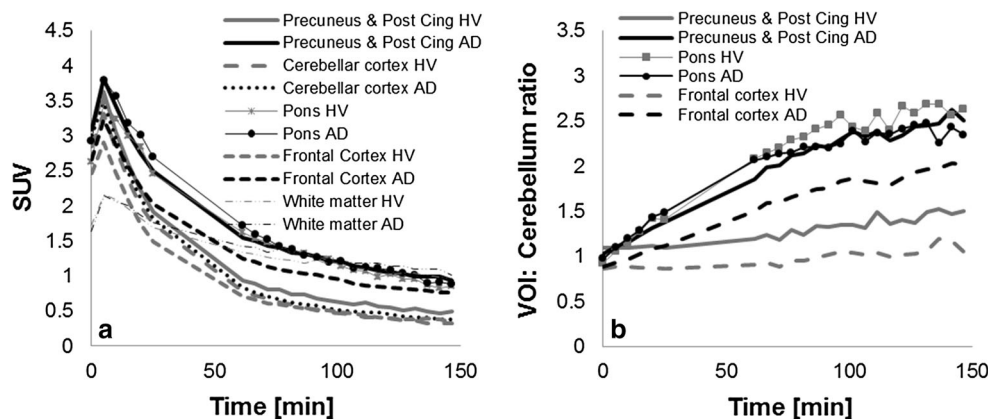


Fig. 2 Time activity curves of AD and HV subjects. **a** Shows average time activity curves for the healthy volunteers (HV, $N = 3$) and AD subjects (AD, $N = 3$) from time of injection to 150 min post-injection in the outlined region covering posterior cingulate and precuneus,

pons, frontal cortex, white matter and the cerebellar cortex. In **b** the ratio of the posterior cingulate and precuneus, frontal cortex, and pons over cerebellar cortex for the two groups is shown

Table 2 Regional DVRs and SUVRs of [¹⁸F]flutemetamol in probable Alzheimer's disease (AD) patients and healthy volunteers (HV) in Step A

	ANC	FRO	LTC	PAR	POC	SMC	STRI
Reference Logan 60–150 min with cerebellar cortex as reference region							
HV 1	1.097	0.946	0.965	0.983	1.158	0.980	1.227
HV 2	1.278	0.936	1.088	1.091	1.276	1.007	1.467
HV 3	1.174	0.871	1.030	1.014	1.113	1.031	1.329
AD 1	1.727	1.519	1.518	1.533	1.805	1.229	1.837
AD 2	2.013	1.556	1.603	1.720	2.029	1.419	1.788
AD 3	1.735	1.332	1.365	1.508	1.616	1.261	1.734
SUVR (85–115 min) with cerebellar cortex as reference region							
HV 1	1.132	1.069	1.096	1.229	1.390	1.235	1.344
HV 2	1.550	1.030	1.231	1.210	1.425	1.135	1.687
HV 3	1.397	0.978	1.185	1.174	1.252	1.201	1.504
AD 1	2.244	1.960	1.965	2.035	2.368	1.463	2.383
AD 2	2.691	2.079	2.143	2.321	2.751	1.846	2.178
AD 3	2.161	1.550	1.667	1.857	1.962	1.453	2.170

ANC anterior cingulate, FRO frontal cortex, LTC lateral temporal cortex, PAR inferior parietal cortex, POC posterior cingulate and precuneus, SMC sensorimotor cortex, STRI striatum

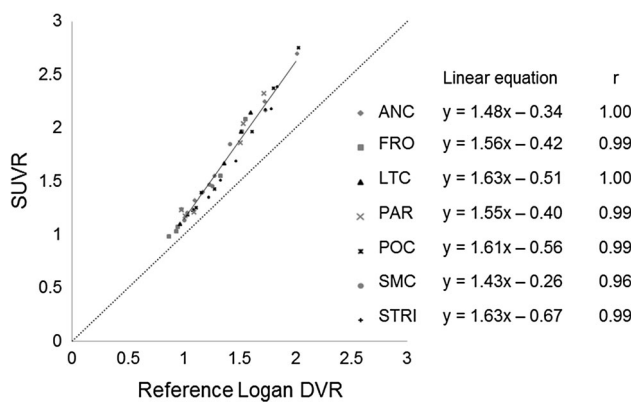


Fig. 3 Correlation plot for cortical regions and striatum for the [¹⁸F]flutemetamol uptake quantified using reference Logan over 60–150 min, and SUVR for 85–115 min with cerebellum as reference region for both methods. ANC anterior cingulate, FRO frontal cortex, LTC lateral temporal cortex, PAR inferior parietal cortex, POC posterior cingulate and precuneus, SMC sensorimotor cortex, STRI striatum

for AD subjects 4, 6 and 7 from the Step B cohort. These three subjects had an uptake pattern similar to that of the HV subjects—a white matter uptake pattern. The mean SUVR for the time window of 85–115 min was significantly raised in nearly all cortical areas in the pooled AD cohort compared with the HV subjects from Step A and B. An exception was the medial temporal cortex which showed little statistical evidence of amyloid deposition ($p = 0.426$). The striatal SUVR was significantly raised in AD ($p = 0.001$) whereas pons and subcortical white matter SUVRs were not ($p = 0.392$ and $p = 0.167$). The composite VOI SUVRs, comprising association cortical regions, was also significantly raised in AD ($p = 0.002$) and this was also seen when using pons as reference region

($p = 0.008$). The SUVRs are visualized graphically in Fig. 5 and the group averages, standard deviations and p values for each region are listed in Table 3.

Population-based comparisons

To avoid bias in the assessment of population based differences, potential outliers with uptake patterns uncharacteristic of the specific subject group were identified visually by an independent reader trained in the visual assessment of [¹⁸F]flutemetamol images. This led to the exclusion of three Japanese AD subjects with normal appearing uptake pattern, two Caucasian AD subjects with normal uptake pattern and one Caucasian HV subject with abnormal uptake pattern. The cohort sizes in the analysis were 5 Japanese AD subjects, 6 Caucasian AD subjects, 8 Japanese HV subjects and 7 Caucasian HV subjects.

There were no statistically significant differences, the range of p values for the different regions was 0.11–0.82 when comparing Japanese HV with Caucasian HV and Japanese AD with Caucasian AD; group averages and SDs computed excluding the outliers are visualized in Fig. 6.

Discussion

This study demonstrated that a standardized uptake value ratio (SUVR) derived from a time window 85–115 min post-injection of [¹⁸F]flutemetamol is successful in distinguishing Japanese subjects with probable AD from healthy controls. Only in one of the eight studied cortical gray matter regions, the medial temporal cortex, could SUVR not statistically differentiate between healthy controls and

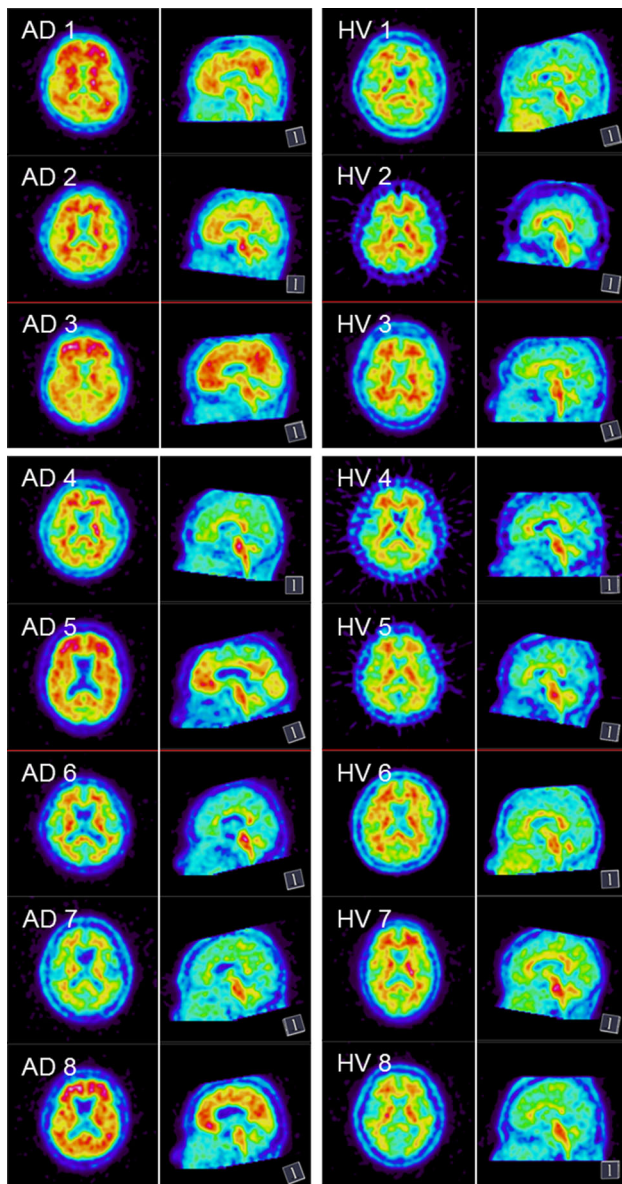


Fig. 4 Axial and sagittal summation images for the pooled Step A and B subjects (85–115 min). Step A (subjects AD 1–3 and HV 1–3) and Step B (subjects AD 4–8 and HV 4–8). Axial images approximately at the level of striatum, sagittal to the side of the midline, showing anterior and posterior cingulate. The image intensity is anchored with pons ~90 % of maximum image activity in all images

subjects with AD. This mirrors the observation in a previously performed study in Caucasian subjects [4] and has also been seen in voxel-based analysis using [^{11}C]PiB [18]. The medial temporal cortex, including hippocampus are greatly affected by atrophy in Alzheimer's disease and the absence of differences may therefore be attributed to mis-registrations to the template space leading to inclusion of cerebrospinal fluid in the outlined VOIs and partial volume effects resulting in a lower uptake estimate in this region

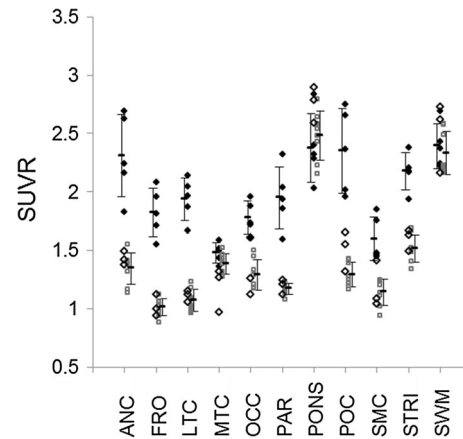


Fig. 5 Pooled data for Steps A and B of the SUVR for 85–115 min using the cerebellar cortex as reference region. The mean and standard deviation for each group (excluding AD outliers) are represented with error bars. Diamonds represent AD subjects, the open diamonds show outliers, i.e., AD subjects 4, 6 and 7. Squares represent healthy volunteers. *ANC* anterior cingulate, *FRO* frontal cortex, *LTC* lateral temporal cortex, *MTC* medial temporal cortex, *OCC* occipital cortex, *PAR* inferior parietal cortex, *PONS* pons, *SMC* sensorimotor cortex, *STRI* striatum, *SWM* subcortical white matter

rather than lack of β -amyloid deposition. Regardless of the underlying mechanism, this region is not reliable in the differentiation of AD subjects from healthy controls using quantitative approaches.

The Caucasian study also demonstrated that SUVRs provide a valid method of uptake quantification by comparing different approaches of kinetic modeling of [^{18}F]flutemetamol [4] as did a recent study comparing brain [^{18}F]flutemetamol uptake in Japanese subjects [10]. [^{18}F]flutemetamol showed a sensitivity of 97.2 % and specificity of 85.3 % for discriminating AD patients from older healthy subjects on visual assessment of PET images with clinical diagnosis as the gold standard [10]. In the previously performed Caucasian study [4], arterial blood sampling was performed in six subjects to enable full kinetic modeling of [^{18}F]flutemetamol uptake. Based on the robust results obtained from the previous study showing that reference region quantification allowed a good discrimination between AD and healthy controls, it was decided to exclude arterial blood sampling in this study, as it is an invasive procedure, creating discomfort for the patient and unsuitable for use in a clinical routine protocol. This present study confirmed that brain tracer uptake kinetics is similar in Caucasian and Japanese subjects and SUVRs a valid method of estimating amyloid load in AD cases.

Our primary analyses were performed using the cerebellar cortex as reference region of non-specific uptake when computing volumes of distribution and SUVRs, as visual comparison of the time-activity curves showed

Table 3 Summary and statistics of group wise comparisons of SUVR using cerebellar cortex as reference region over 85–115 min

Region	AD (<i>N</i> = 8) mean SUVR (SD)	HV (<i>N</i> = 8) mean SUVR (SD)	<i>p</i> value outliers included (<i>N</i> = 16)	<i>p</i> value outliers excluded (<i>N</i> = 13)*
Anterior cingulate	1.980 (0.53)	1.347 (0.14)	0.003	0.003
Frontal cortex	1.522 (0.45)	1.014 (0.07)	0.003	<0.001
Lateral temporal cortex	1.628 (0.45)	1.073 (0.09)	0.002	<0.001
Medial temporal cortex	1.371 (0.19)	1.385 (0.09)	0.426	0.040
Occipital cortex	1.612 (0.29)	1.290 (0.13)	0.006	<0.001
Inferior parietal cortex	1.667 (0.44)	1.173 (0.05)	0.003	<0.001
Pons	2.518 (0.31)	2.482 (0.21)	0.392	0.230
Posterior cingulate and precuneus	2.035 (0.52)	1.293 (0.11)	0.001	<0.001
Sensorimotor cortex	1.442 (0.28)	1.143 (0.11)	0.007	<0.001
Striatum	1.959 (0.32)	1.517 (0.12)	0.001	<0.001
Subcortical white matter	2.434 (0.22)	2.331 (0.18)	0.167	0.291

* An estimation of the AD group average was also made excluding the three subjects with uptake pattern resembling the typical pattern when no amyloid accumulation is present for comparison

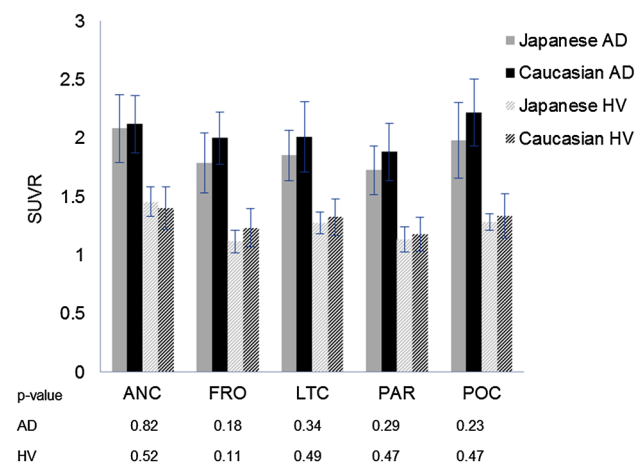


Fig. 6 Group averages of SUVR using cerebellar cortex as reference region over 80–90 min for the AD and HV of the Japanese and Caucasian population excluding outliers, the *t* test *p* value for each group comparison is included. *ANC* anterior cingulate, *FRO* frontal cortex, *LTC* lateral temporal cortex, *PAR* inferior parietal cortex, *POC* posterior cingulate and precuneus

similar cerebellar [¹⁸F]flutemetamol uptake in healthy and AD subjects. The pons also appeared to provide a valid reference region indicating its appropriateness for use as an option if the patient positioning in the scanner has resulted in the cerebellum being outside the field-of-view.

Measuring the SUVR over different time windows showed a slight increase with time in the AD group, likely due to wash out of free radiotracer from the blood compartment in cerebellar cortex. In clinical settings the impact of this increase in SUVR over time would be negligible, as long as a consistent scanning protocol is used. The exact choice of late scanning window had no effect on the visual

appearance of the image data which is the primary means for classifying the uptake in a clinical setting.

While the standardized use of [¹⁸F]flutemetamol for clinical assessment of β -amyloid deposition will most likely be based on a visual assessment, quantitative analysis using SUVR can still be supportive especially in equivocal cases. It is also likely that clinical use of [¹⁸F]flutemetamol would not include an early phase PET scan or an MR scan as part of the examination, which is a challenge to placement of VOIs. However, a methodology for spatially normalizing [¹⁸F]flutemetamol images by means of an adaptive [¹⁸F]flutemetamol specific template [19] has enabled the automated quantification with a 91 % sensitivity and 88 % specificity when compared to visual assessments [20].

This was the first [¹⁸F]flutemetamol study to assess the kinetics of the tracer in an all-Japanese cohort and compare these with historical Caucasian subjects. It has been shown here that there are no significant differences in the uptake characteristics of [¹⁸F]flutemetamol between these Japanese cohorts and the Caucasian cohorts from the previous Phase I study. Due to the small number of subjects and exclusion of outliers, the statistical test in the present study does not provide strong evidence but may be sufficient to support the applicability of already-validated [¹⁸F]flutemetamol to Japanese population.

This comparison was made excluding the AD subjects with apparently normal uptake pattern in the AD groups (three in the Japanese cohort, two in the Caucasian) and healthy controls with an abnormal uptake pattern in the HV group (one in the Caucasian cohort) based on the visual appearance of the [¹⁸F]flutemetamol images. A probable explanation for the absence of raised [¹⁸F]flutemetamol uptake in the five AD subjects is that these in fact suffer

from either a dementia that is unrelated to accumulation of β -amyloid or a non-degenerative cause for their impaired neuropsychological and clinical ratings on testing. The proportion of cognitively intact elderly subjects that show incidental elevated [^{11}C]PiB uptake has been noted to be around 10–30 % depending on age [21–26] and the Caucasian subject with an uptake pattern similar to that of AD subjects is likely to be part of this group.

This study has shown that [^{18}F]flutemetamol uptake can be quantified in Japanese subjects using a simplified SUVR approach and that cortical SUVRs can discriminate between probable AD patients and healthy controls. The results are similar to those seen in Caucasian populations and indicate that there are no significant differences in the behavior of [^{18}F]flutemetamol between the two populations.

Acknowledgments The authors would like to thank the participating centers for contributing to the study with their knowledge, time and effort. We would also like to express our gratitude to the volunteering patients and their families, and healthy control subjects for participating in our study. The authors could also like to thank all the contributors at GE Healthcare. This work was entirely funded by GE Healthcare.

References

1. Sekita A, Ninomiya T, Tanizaki Y, Doi Y, Hata J, Yonemoto K, et al. Trends in prevalence of Alzheimer's disease and vascular dementia in a Japanese community: the Hisayama Study. *Acta Psychiatr Scand*. 2010;122:319–25.
2. Prince M, Bryce R, Albanese E, Wimo A, Ribeiro W, Ferri CP. The global prevalence of dementia: a systematic review and metanalysis. *Alzheimers Dement*. 2013;9:63–75.
3. American Psychiatric Association. Diagnostic and statistical manual of mental disorders DSM-IV. 4th Edn, 1994.
4. Nelissen N, Van Laere K, Thurfjell L, Owenius R, Vandenbulcke M, Koole M, et al. Phase I study of the Pittsburgh compound B derivative [^{18}F]flutemetamol in healthy volunteers and patients with probable Alzheimer disease. *J Nucl Med*. 2009;50:1251–9.
5. Koole M, Lewis DM, Buckley C, Nelissen N, Vandenbulcke M, Brooks DJ, et al. Whole-body distribution and radiation dosimetry of [^{18}F]flutemetamol: a radioligand for in vivo brain amyloid imaging. *J Nucl Med*. 2009;50:818–22.
6. Vandenberghe R, Van Laere K, Ivanoiu A, Salmon E, Bastin C, Triau E, et al. [^{18}F]flutemetamol amyloid imaging in Alzheimer disease and mild cognitive impairment: a phase 2 trial. *Ann Neurol*. 2010;68:319–29.
7. Thurfjell L, Lötjönen J, Lundqvist R, Koikkalainen J, Soininen H, Waldemar G, et al. Combination of biomarkers: PET [^{18}F]flutemetamol imaging and structural MRI in dementia and mild cognitive impairment. *Neurodegener Dis*. 2012;10:246–9.
8. Rinne JO, Frantzen J, Leinonen V, Lonrot K, Laakso A, Virtanen KA, et al. Prospective Flutemetamol Positron Emission Tomography and Histopathology in Normal Pressure Hydrocephalus. *Neurodegener Dis*. 2014;13:237–45.
9. Wolk DA, Grachev ID, Buckley C, Kazi H, Grady MS, Trojanowski JQ, et al. Association between in vivo fluorine 18-labeled flutemetamol amyloid positron emission tomography imaging and in vivo cerebral cortical histopathology. *Arch Neurol*. 2011;68:1398–403.
10. Hatashita S, Yamasaki H, Suzuki Y, Tanaka K, Wakebe D, Hayakawa H. [^{18}F]flutemetamol amyloid-beta PET imaging compared with [^{11}C]PiB across the spectrum of Alzheimer's disease. *Eur J Nucl Med Mol Imaging*. 2014;41:290–300.
11. Andersson J, Thurfjell L. Implementation and validation of a fully automatic system for intra- and interindividual registration of PET brain scans. *J Comput Assist Tomogr*. 1997;21:136–44.
12. Lammertsma AA, Bench CJ, Price GW, Cremer JE, Luthra SK, Turton D, et al. Measurement of cerebral monoamine oxidase B activity using L-[^{11}C]deprenyl and dynamic positron emission tomography. *J Cereb Blood Flow Metab*. 1991;11:545–56.
13. Logan J, Fowler JS, Volkow ND, Wolf AP, Dewey SL, Schlyer DJ, et al. Graphical analysis of reversible radioligand binding from time-activity measurements applied to [^{11}C -methyl]-(-)-cocaine PET studies in human subjects. *J Cereb Blood Flow Metab*. 1990;10:740–7.
14. Logan J, Fowler JS, Volkow ND, Wang GJ, Ding YS, Alexoff DL. Distribution volume ratios without blood sampling from graphical analysis of PET data. *J Cereb Blood Flow Metab*. 1996;16:834–40.
15. Lopresti BJ, Klunk WE, Mathis CA, Hoge JA, Ziolkowski SK, Lu X, et al. Simplified quantification of Pittsburgh compound B amyloid imaging PET studies: a comparative analysis. *J Nucl Med*. 2005;46:1959–72.
16. Camus V, Payoux P, Barré L, Desgranges B, Voisin T, Tauber C, et al. Using PET with [^{18}F]florbetapir to quantify brain amyloid load in a clinical environment. *Eur J Nucl Med Mol Imaging*. 2012;39:621–31.
17. Becker GA, Ichise M, Barthel H, Luthardt J, Patt M, Seese A, et al. PET quantification of [^{18}F]florbetapir binding to β -amyloid deposits in human brains. *J Nucl Med*. 2013;54:723–31.
18. Kempainen NM, Aalto S, Wilson IA, Nägren K, Helin S, Brück A, et al. Voxel-based analysis of PET amyloid ligand [^{11}C]PiB uptake in Alzheimer disease. *Neurology*. 2006;67:1575–80.
19. Lundqvist R, Lilja J, Thomas BA, Lötjönen J, Villemagne VL, Rowe CC, et al. Implementation and validation of an adaptive template registration method for [^{18}F]flutemetamol imaging data. *J Nucl Med*. 2013;54:1472–8.
20. Thurfjell L, Lilja J, Lundqvist R, Buckley C, Smith A, Vandenberghe R, et al. Automated quantification of [^{18}F]flutemetamol PET activity for categorizing scans as negative or positive for brain amyloid: concordance with visual image reads. *J Nucl Med*. 2014;55:1623–8.
21. Klunk WE, Engler H, Nordberg A, Wang Y, Blomqvist G, Holt DP, et al. Imaging brain amyloid in Alzheimer's disease with Pittsburgh compound-B. *Ann Neurol*. 2004;55:306–19.
22. Mintun MA, Larossa GN, Sheline YI, Dence CS, Lee SY, Mach RH, et al. [^{11}C]PiB in non-demented population: a potential antecedent marker of Alzheimer's disease. *Neurology*. 2006;67:446–52.
23. Pike KE, Savage G, Villemagne VL, Ng S, Moss SA, Maruff P, et al. Beta-amyloid imaging and memory in non-demented individuals: evidence for preclinical Alzheimer's disease. *Brain*. 2007;130:2837–44.
24. Aizenstein HJ, Nebes RD, Saxton JA, Price JC, Mathis CA, Tsopelas ND, et al. Frequent amyloid deposition without significant cognitive impairment among the elderly. *Arc Neurol*. 2008;65:1509–17.
25. Jack CR Jr, Lowe VJ, Senjem ML, Weigand SD, Kemp BJ, Shiung MM, et al. [^{11}C]PiB and structural MRI provide complementary information in imaging of Alzheimer's disease and amnesic mild cognitive impairment. *Brain*. 2008;131:665–80.
26. Mormino EC, Kluth JT, Madison CM, Rabinovici GD, Baker SL, Miller BL, et al. Episodic memory loss is related to hippocampal-mediated beta-amyloid deposition in elderly subjects. *Brain*. 2009;132:1310–23.